

## Direct Visualization of Lipid Phase Segregation in Single Lipid Bilayers with Coherent Anti-Stokes Raman Scattering Microscopy

Eric O. Potma and X. Sunney Xie<sup>\*[a]</sup>

Lipid rafts, segregated domains with different lipid compositions, are thought to play crucial roles in processes such as protein sorting and signaling on cell membranes.<sup>[1–3]</sup> Despite their postulated importance in membrane biology, direct observation of lipid rafts in cells remains a challenge. To deepen the understanding of the chemical and physical characteristics of segregated lipid phase domains, model membrane systems have been extensively used. Supported mono- and bilayers of binary mixtures of phosphatidylcholines have segregated phase domains varying from tens of nanometers to several microns in size, which were revealed by atomic force microscopy<sup>[4,5]</sup> and fluorescence microscopy.<sup>[6,7]</sup> To eliminate the effects of geometrical constraints on domain formation, free-standing bilayers in the form of giant unilamellar vesicles (GUV) have been used as models for the cell membrane. Micrometer-sized domain structures have been seen in mixed bilayers of various phospholipids<sup>[8,9]</sup> and in mixtures of phospholipids with sphingolipids.<sup>[7,10]</sup> Using the GUV model system, membrane phase diagrams have been obtained for ternary mixtures of saturated lipids, unsaturated lipids and cholesterol.<sup>[10–12]</sup> The vesicle system has also proven suitable for membrane fluidity measurements<sup>[8,10]</sup> and the determination of membrane tension and curvature at phase domain boundaries.<sup>[13]</sup>

Lipid phase separation in free-standing bilayers, however, has not been directly observed. Visualization of the different phases requires the addition of fluorescent compounds that have either a different affinity for the distinct lipid domains or a lipid environment-dependent fluorescence response.<sup>[7]</sup> Variations in probe partitioning or photophysical changes not directly related to lipid phase domains can obscure a correct assignment of membrane morphology. In addition, it is generally assumed that interactions of the probes with the lipids are minor and not affecting the formation of segregated domains. Nevertheless, at concentrations up to a few mole percent, perturbing interactions cannot be completely ruled out.<sup>[14]</sup> In a multicomponent system such as that of lipid membranes, small traces of charged or polar foreign molecules may distort the thermodynamics and kinetics of lipid phase segregation in bilayers. To rule out any artifacts, a clear visualization of lipid domains in free-standing bilayers without the addition of fluorescent labels is required for an unambiguous observation of phase-segregated lipid domains.

[a] E. O. Potma, Prof. X. S. Xie  
Department of Chemistry and Chemical Biology  
Harvard University, 12 Oxford Street, Cambridge  
Massachusetts 02138 (USA)  
Fax: (+1) 617-496-8709  
E-mail: xie@chemistry.harvard.edu

Here we use coherent anti-Stokes Raman scattering (CARS) microscopy for imaging of giant vesicles of binary mixtures of lipids. The vibrational selectivity of the CARS microscope allows identification of molecules based on spectroscopic signatures.<sup>[15]</sup> The sensitivity of CARS vibrational imaging has previously been shown to be high enough to visualize single lipid bilayers.<sup>[16,17]</sup> In this contribution we show that in bilayers composed of binary mixtures of phospholipids, individual components can be visualized with chemical selectivity.

Two synchronized picosecond Ti:sapphire lasers were used for delivery of the pump and the Stokes beams in the CARS excitation process.<sup>[18]</sup> The pump beam was set to 711.0 nm ( $14064\text{ cm}^{-1}$ ) while the Stokes beam was varied between 831.6 nm ( $12025\text{ cm}^{-1}$ ) and 838.6 nm ( $11924\text{ cm}^{-1}$ ). The pulse duration was about 3 ps, corresponding to a spectral width of  $\approx 5\text{ cm}^{-1}$ . A beam scanning microscope was employed for raster scanning of the sample. Signals were detected in the forward (F-CARS) direction through three bandpass filters (630 nm, 40 nm bandwidth). Scan times were typically 10 s per image with average beam powers of 25 mW at a pulse repetition rate of 82 MHz. To relate the acquired CARS images of mixed lipid bilayers to the typical results obtained with fluorescent probes, we have supplemented the CARS microscope with a module for simultaneous detection of two-photon excited fluorescence. The membrane probe *N*-lissamine rhodamine dipalmitoylphosphatidyl-ethanolamine (rho-DPPE), which accumulates preferentially in one of the lipid phases, was used at concentrations not higher than 1 mole% to visualize lipid phase segregation. The probe was two-photon excited with the pump and Stokes picosecond-pulses, and epi-fluorescence was detected through a bandpass filter centered at 600 nm.

GUVs composed of 1,2-dioleoyl-*sn*-glycero-3-phosphocholine (DOPC) and 1,2-distearoyl-*sn*-glycero-3-phosphocholine (DSPC) (0.5/0.5 molar ratio) were used in this study. At room temperature, DOPC assumes a liquid-disordered phase whereas DSPC resides in a gel phase. GUVs were prepared with the electroformation method.<sup>[19]</sup> Lipid mixtures dissolved in chloroform/methanol (9:1) were dried on platinum electrodes, after which millipore water was added. Unilamellar vesicles were formed by applying 2 V at 10 Hz for 90 minutes. Measurements were done at room temperature. No significant movements or undulations of the bilayer vesicles were observed during image acquisition.

Lipids can be conveniently visualized through the CH-stretching vibrations of the acyl chains, which give rise to a strong Raman band around  $2845\text{ cm}^{-1}$ . Although DOPC and DSPC display spectral differences in the CH-stretching vibrational range, these differences yield only a small contrast for imaging.<sup>[20,21]</sup> To increase contrast, deuterated lipids can be used.<sup>[22]</sup> A mixture was made of regular DOPC with deuterated  $[D_{70}]$ DSPC in which 70 hydrogen atoms have been replaced by deuterium atoms. The corresponding  $CD_2$  stretch vibration ( $2100\text{ cm}^{-1}$ ) is red-shifted with respect to the CH-stretching vibrations, allowing an uncontaminated detection of  $[D_{70}]$ DSPC, as shown in the Raman spectrum of Figure 1. The CARS spectrum follows the same trend as the Raman spectrum, with the strongest signal at  $2090\text{ cm}^{-1}$ . Hence, when setting the Raman

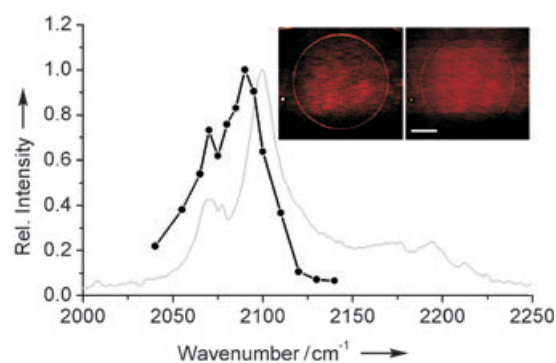


**Figure 1.** Raman (grey line) and CARS (black dots) spectra of deuterated DSPC ( $[D_{70}]$ DSPC). The CARS spectrum shows a characteristic red-shift relative to the Raman spectrum. In the inset, the left panel shows a CARS image of a  $[D_{70}]$ DSPC giant unilamellar vesicle recorded at  $2090\text{ cm}^{-1}$ , the right panel shows the same vesicle imaged at  $2140\text{ cm}^{-1}$ . Images were recorded at room temperature ( $21^\circ\text{C}$ ). Scale bar is  $10\text{ }\mu\text{m}$ .

shift to  $2090\text{ cm}^{-1}$ , strong resonant signals are expected for  $[D_{70}]$ DSPC whereas DOPC has no resonant response in this spectral range. The inset of Figure 1 shows CARS images of  $[D_{70}]$ DSPC vesicles when tuning in and out of resonance. From the images it can be clearly seen that the vibrational signal represents an excellent chemical marker for the vesicles. In addition to the vibrationally resonant signal, a nonresonant electronic contribution from the surrounding water is observed. Despite the large offset introduced by the nonresonant water signal, about ten times the vibrationally resonant signal, the resonant signal from the lipid is easily discerned. When tuning away from the resonance frequency, a weak signal from the bilayer still remains, which is due to the nonresonant signal from the phospholipids.

We first verified the existence of lipid phase domains in labeled DOPC/ $[D_{70}]$ DSPC vesicles. Phase-segregated domains are observed in the CARS images taken at the  $CD_2$  Raman band (Figure 2a). The existence of lipid domains is furthermore confirmed in the simultaneously recorded two-photon fluorescence images (Figure 2b). The morphology of the domains is similar to the patterns observed in previous fluorescence stud-

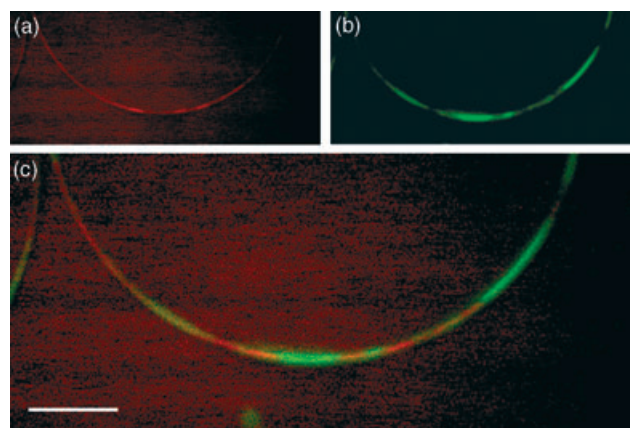


**Figure 2.** Simultaneous CARS and two-photon fluorescence imaging of 1:1 DOPC: $[D_{70}]$ DSPC GUVs with 1% rho-DPPE. a) CARS image at  $2090\text{ cm}^{-1}$ ; b) Fluorescence image; c) Overlay of (a) and (b). Scale bar is  $5\text{ }\mu\text{m}$ .

ies, which indicates that deuteration of the acyl chains does not alter the thermodynamic state of the lipid domains in this system. The bright zones in the CARS image correspond to regions rich in  $[D_{70}]$ DSPC, the dark regions represent membrane parts low in  $[D_{70}]$ DSPC. The CARS image is complementary to the fluorescence image, as shown in the overlay in Figure 2c. From this image, it is evident that the fluorescence probe partitions preferentially in the liquid-disordered phase of DOPC, as previously reported.<sup>[23]</sup>

A direct CARS visualization of lipid domains without fluorescent markers is given in Figure 3. Along the membrane, bright patches are seen on the bilayer background signal. The pat-

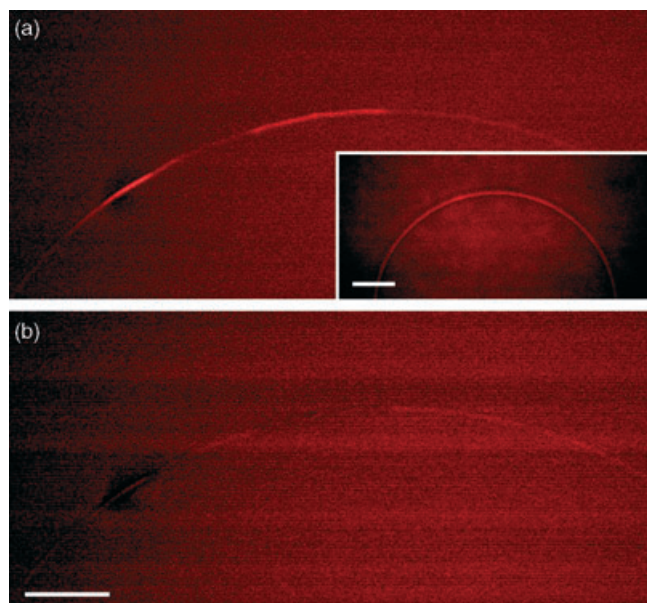


**Figure 3.** CARS images of part of an unstained GUV of binary mixture 1:1 DOPC/ $[D_{70}]$ DSPC. a) On resonance with  $[D_{70}]$ DSPC at  $2090\text{ cm}^{-1}$  showing a sharp phase segregation of the lipids. Inset shows a vesicle of 1:1 DOPC/ $[D_{70}]$ DSPC with 10% cholesterol, in which the clear pattern is absent. b) Similar vesicle as in (a) recorded off-resonance with  $[D_{70}]$ DSPC at  $2140\text{ cm}^{-1}$ . Note that the bright signal from  $[D_{70}]$ DSPC completely vanishes. Scale bars are  $5\text{ }\mu\text{m}$ .

terns observed are similar to the domain structures seen in the dye-labeled system. By tuning in and out of the  $\text{CD}_2$  vibrational resonance, we concluded that the bright zones reflect a high concentration of  $[D_{70}]$ DSPC. Whereas in fluorescence studies the signal intensity depends on the complicated partitioning characteristics of the probe, in CARS microscopy the signal strength directly reflects the concentration of the lipids. Comparison of the signal levels in Figure 3 with the signal levels of the vesicles of pure DOPC or  $[D_{70}]$ DSPC reveals that the bright zones in Figure 3 are almost exclusively composed of  $[D_{70}]$ DSPC. More generally, a calibration curve can be calculated from which the relative concentration of the different lipids can be deduced.<sup>[24]</sup> As shown in the inset of Figure 3a, addition of 10% cholesterol dissolves the clear domain patterns, corroborating previous fluorescence experiments.<sup>[23]</sup>

In conclusion, we have shown that CARS microscopy provides a nonperturbative way of probing the existence and morphology of phase-segregated lipid domains, circumventing

perturbations, photobleaching and assignment problems associated with the use of fluorescent probes. Our results unambiguously reveal the formation of domains in binary mixtures of saturated and unsaturated phospholipids previously studied using fluorescence microscopy. CARS microspectroscopic mapping of the vibrational bands can furthermore uncover molecular information of the different domains.<sup>[17]</sup> Omitting the use of fluorescent markers, CARS microscopy holds great promise as a method of studying lipid rafts in cells.

## Acknowledgements

This work was supported by an NSF grant (DBI-0138028) and an NIH grant (GM62536-01). E.O.P. acknowledges financial support from the European Molecular Biology Organization (EMBO).

**Keywords:** CARS (coherent anti-Stokes Raman scattering) · fluorescence · phospholipids · vesicles · vibrational spectroscopy

- [1] D. A. Brown, E. London, *J. Biol. Chem.* **2000**, *275*, 17221–17224.
- [2] K. Simons, E. Ikonen, *Nature* **1997**, *387*, 567–572.
- [3] H. M. McConnell, M. Vrljic, *Annu. Rev. Biophys. Biomol. Struct.* **2003**, *32*, 469–492.
- [4] P. Moraille, A. Badia, *Langmuir* **2002**, *18*, 4414–4419.
- [5] F. Tokumasu, A. J. Jin, G. W. Feigenson, J. A. Dvorak, *Biophys. J.* **2003**, *84*, 2609–2618.
- [6] H. M. McConnell, *Annu. Rev. Phys. Chem.* **1991**, *42*, 171–195.
- [7] C. Dietrich, L. A. Bagatolli, Z. N. Volovyk, N. L. Thompson, M. Levi, K. Jacobson, E. Gratton, *Biophys. J.* **2001**, *80*, 1417–1428.
- [8] J. Korlach, P. Schwille, W. W. Webb, G. W. Feigenson, *Proc. Natl. Acad. Sci. USA* **1999**, *96*, 8461–8466.
- [9] L. A. Bagatolli, E. Gratton, *Biophys. J.* **2000**, *78*, 290–305.
- [10] N. Kahya, D. Scherfeld, K. Bacia, B. Poolman, P. Schwille, *J. Biol. Chem.* **2003**, *278*, 28109–28115.
- [11] G. W. Feigenson, J. T. Buboltz, *Biophys. J.* **2001**, *80*, 2775–2788.
- [12] S. L. Veatch, S. L. Keller, *Biophys. J.* **2003**, *85*, 3074–3083.
- [13] T. Baumgart, S. T. Hess, W. W. Webb, *Nature* **2003**, *425*, 821–824.
- [14] M. Hao, F. R. Maxfield, *J. Fluoresc.* **2001**, *11*, 287–295.
- [15] J.-X. Cheng, X. S. Xie, *J. Phys. Chem. B* **2004**, *108*, 827–840.
- [16] E. O. Potma, X. S. Xie, *J. Raman Spectrosc.* **2003**, *34*, 642–650.
- [17] G. W. H. Wurpel, J. M. Schins, M. Muller, *J. Phys. Chem. B* **2004**, *108*, 3400–3403.
- [18] E. O. Potma, D. J. Jones, J. X. Cheng, X. S. Xie, J. Ye, *Opt. Lett.* **2002**, *27*, 1168–1170.
- [19] M. I. Angelova, D. S. Dimitrov, *Faraday Discuss. Chem. Soc.* **1986**, *81*, 303–308.
- [20] J.-X. Cheng, A. Volkmer, L. D. Book, X. S. Xie, *J. Phys. Chem. B* **2002**, *106*, 8493–8498.
- [21] M. Muller, J. M. Schins, *J. Phys. Chem. B* **2002**, *106*, 3715–3723.
- [22] G. R. Holtom, B. D. Thrall, B.-Y. Chin, H. S. Wiley, S. D. Colson, *Traffic* **2001**, *2*, 781–788.
- [23] D. Scherfeld, N. Kahya, P. Schwille, *Biophys. J.* **2003**, *85*, 3758–3768.
- [24] A calibration curve can be calculated based on the known quadratic CARS signal dependence on the concentration, under the assumption that the vibrational spectra of the lipids remain invariant for different mixture ratios. In addition, for an accurate determination of the concentration, knowledge is required on the real and imaginary parts of the CARS spectrum. This information can be obtained from CARS spectral measurements.

Received: August 16, 2004

Early View Article  
Published online on December 9, 2004